

PAPER • OPEN ACCESS

## Optimisation of Pelton turbine jet deflector using CFD analysis

To cite this article: Boro Popovski *et al* 2019 *IOP Conf. Ser.: Earth Environ. Sci.* **240** 022031

View the [article online](#) for updates and enhancements.



**IOP | ebooks™**

Bringing you innovative digital publishing with leading voices to create your essential collection of books in STEM research.

Start exploring the [collection](#) - download the first chapter of every title for free.

# Optimisation of Pelton turbine jet deflector using CFD analysis

**Boro Popovski<sup>1</sup>, Andrej Lipej<sup>2</sup>, Zoran Markov<sup>1</sup>, Predrag Popovski<sup>1</sup>**

<sup>1</sup>University Ss Cyril and Methodius, Faculty of Mechanical Engineering, Skopje, Macedonia

<sup>2</sup>University of Novo mesto, Faculty of Mechanical Engineering, Slovenia

**Abstract.** The high head Pelton turbines operate with extreme conditions. In case to need a sudden stop of operation, one of the important parts is jet deflector, which can be in push-out, or cut-of options. The paper presents the optimisation procedure of Pelton Turbine push-out jet deflector shape using numerical simulation of three-dimensional turbulent flow in order to minimize the forces, stresses, deformations and torque of jet deflector servomotor. The calculations are performed using the CFD package Ansys CFX. The steps for flow modelling, 3-D geometry definition, mesh generation, pre-processing and post-processing, as well as the optimised results obtained from the numerical simulation of the flow in the jet-deflector are presented. The work corresponds with the actual approach of methods development for flow simulation and calculations of Pelton Turbines. The kinematic and dynamic flow parameters are calculated based on CFD simulations. The results of the calculations represents reliable tool in the procedure of development and construction of Pelton Turbines parts.

## 1 Introduction

For more than 30 years, Computational Fluid Dynamics (CFD) has played an important role in the characteristics improvement of axial and radial water turbines. The relative results of different hydraulic shape modifications on the characteristics curves can be very accurate predicted. Usually the prediction of the absolute values of various characteristics is still a challenge. Another huge problem is a very complex flow analysis of the two phases and free surface flow in Pelton turbine. In the paper, we present an example where results of steady state CFD analysis can be useful tool to successful optimization of some parts of Pelton turbine.

The purpose of this study is to find an accurate numerical procedure that would be capable of accurate predicting of optimal shape and position of closed jet deflector.

Two-phase flow (water and air) in Pelton turbines is always turbulent and unsteady. In this study, we would like to obtain reasonable results by steady state analysis. However, the free surface flow analysis cannot be avoided and has to be modelled by a multiphase model. Numerical analysis of flow in a Pelton turbine is therefore quite complex and time consuming.

In the last fifteen years, many papers about numerical and experimental analysis of flow in Pelton turbines have been published. A water jet from a Pelton turbine injector was presented based on experimental and numerical results in [1]. The influence of secondary velocity fields on jet shape and the influence of jet quality on turbine efficiency were investigated numerically and experimentally [2, 3]. A bucket flow simulation using three adjacent buckets was shown by Mack and Moser in [4]. Kvinsky et al. [5] did one of the first attempts to calculate free surface flow in a rotating bucket. Parkinson et al. [6] presented unsteady analysis of a Pelton runner with flow and mechanical simulation; numerical results were validated by pressure measurements on runner buckets, flow visualization and efficiency measurements. Perrig [7] did the most complete analysis of flow in Pelton turbines. Flow in buckets was investigated through unsteady onboard wall pressure measurements, high-speed onboard



and external flow visualizations, water film thickness measurements and CFD simulations. Recent experimental and numerical investigations put full attention on the influence of nozzle geometry and secondary flow on the jet quality [8], [9]. Based on numerical and experimental results mentioned above, a mass of new knowledge about dynamic process in Pelton turbine was obtained but, still there is no any paper about deflector flow analysis.

## 2 Free surface flow modelling

Free surface flows refer to a multiphase situation where the fluids are separated by a distinct resolvable interface. They can be modelled via a homogeneous or inhomogeneous model. The inhomogeneous model should be used when two fluids are being mixed and later separated. For Pelton turbines the homogeneous model is usually used. Slightly better results can be obtained with the inhomogeneous model, but at a higher cost. In this paper, homogeneous model was used.

The homogeneous model assumes that the transported quantities (with the exception of volume fraction) for the process are the same over all phases.

$$U_\alpha = U, p_\alpha = p, 1 \leq \alpha \leq N_p \quad (1)$$

It is therefore sufficient to solve bulk transport equations for shared fields instead of solving individual transport equations.

$$\frac{\partial \rho}{\partial t} + \nabla \cdot (\rho U) = \sum_{\beta=1}^{N_p} \Gamma_{\alpha\beta} \quad (2)$$

$$\frac{\partial}{\partial t} (\rho U) + \nabla \cdot (\rho U \otimes U - \mu (\nabla U + (\nabla U)^T)) = S_M - \nabla p \quad (3)$$

$\Gamma_{\alpha\beta}$  in equation (2) is the mass flow rate per unit of volume from phase  $\beta$  to phase  $\alpha$ . Density and viscosity are calculated from density and viscosity of all phases in the fluid:

$$\rho = \sum_{\alpha=1}^{N_p} r_\alpha \rho_\alpha, \quad \mu = \sum_{\alpha=1}^{N_p} r_\alpha \mu_\alpha. \quad (4)$$

A detailed description of multiphase models and modelling of free surface flows can be found in [10]. The near-wall modelling is based on the wall-function approach as an extension of the method of Launder and Spalding. In the log-law region the near wall tangential velocity is related to the wall-stress  $\tau_w$ , by means of a logarithmic function. The logarithmic relation for the near wall velocity is given by:

$$u^+ = \frac{U_t}{u_\tau} = \frac{1}{k} \ln(y^+) + C \quad (5)$$

The definition of the  $y^+$  variable is given by the standard definition of  $y^+$  generally used in CFD modelling,

$$y^+ = \frac{\rho \Delta y u_\tau}{\mu} \quad (6)$$

Where  $\Delta n$  is the distance between the first and second grid points off the wall.

## 3 Numerical analysis

The geometry and computational domain of the study case analysed in this paper are presented in figure 1. The geometry consists of complete nozzle with all details and jet deflector. The size of free surface area in the computational domain has been defined in connection with reflected water jet from the deflector. As a first step, an analysis has been done for three different computational grids of the jet deflector domain. Detail data about deflector computational grids at closed position are presented in table 1.

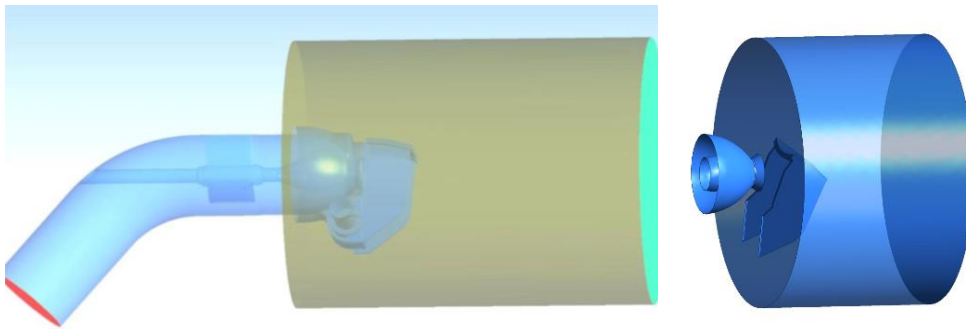


**Figure 1:** Nozzle and deflector geometry (left) and computational domain (right)

**Table 1.** Mesh data for different deflector grids

Grid	Number of elements [mil]	Number of nodes [mil]
Basic grid	14,7	9,6
Refinement 1	17,1	10,4
Refinement 2	18,6	10,8

The quality of computational grid is an important pre-condition for accurate numerical flow analysis results, particularly in case of free surface flow analysis. Automatic grid refinement method is used to accurately predict the water jet from the nozzle. The coarse grid is in the area of water and air but near the border between water and air, the grid is refined. The grid refinement is clearly shown in fig. 2. Grid refinement is also very important in the area where the jet is exiting the nozzle. Besides on the grid refinement near water-air boundary, the special attention has been done also on quality grid near the walls (values of  $y^+$ ). Numerical analysis of the flow in Pelton turbine deflector has been carried out by steady state numerical methods using turbulent model  $k-\omega$  SST and Ansys CFX software package.

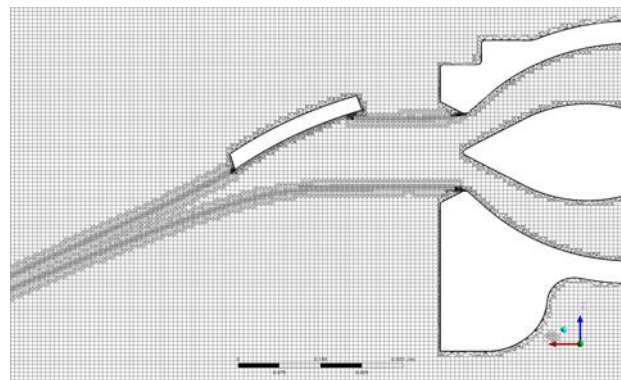


**Figure 2:** Computational grid at closed position

The comparison of CFD results was made for the following flow parameters for the deflector top plate: velocity field, pressure field and  $y^+$  parameter. The quality and convergence of the results for refinement grids was much better in comparison with the basic grid results. The maximal values of  $y^+$  parameters for basic and refinement grids are shown in the table 2.

Table 2. The values at  $y^+$  parameter

Grid	$y^+$
Basic grid	150
Refinement	50

The distribution of  $y^+$  parameter on the upper plate of the jet deflector is presented in the next figure:

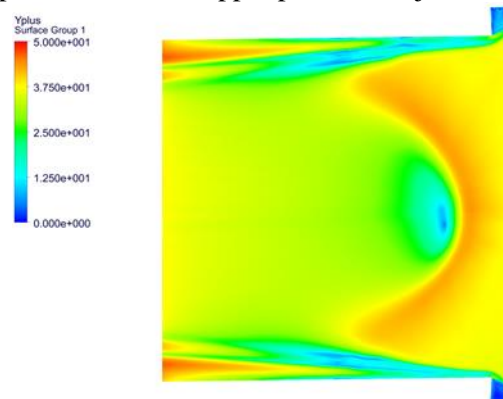


**Figure 3:** Distribution of  $y^+$  values

Based on the analysis of the flow parameters and the results specified above, for further CFD calculation the grid named as Refinement 1 was accepted for further calculations and analysis [11].

## 4 CFD results

### 4.1 Parameters of the basic solution

As a basic solution for prediction of the optimal angular position of the top plate a jet deflector of high head Pelton turbine with rated head of 520 m, maximal discharge of 1,5 m<sup>3</sup>/sec and nozzle outlet diameter of 162 mm was accepted [11].

The water volume fraction for the basic solution is shown in fig. 4. As we can see, two-phase flow is dominant in the thin surface of the jet with the air content of 30 to 70 percent, without jet distortion.

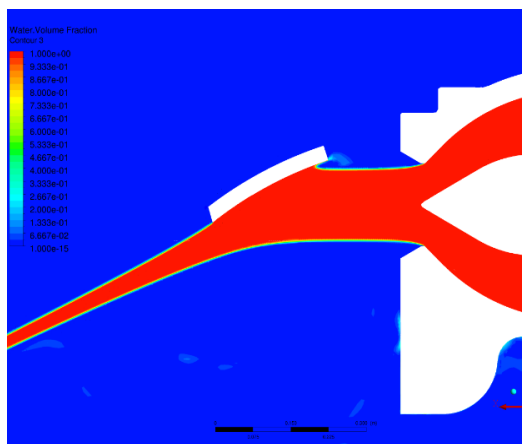


**Figure 4:** Jet water volume fraction

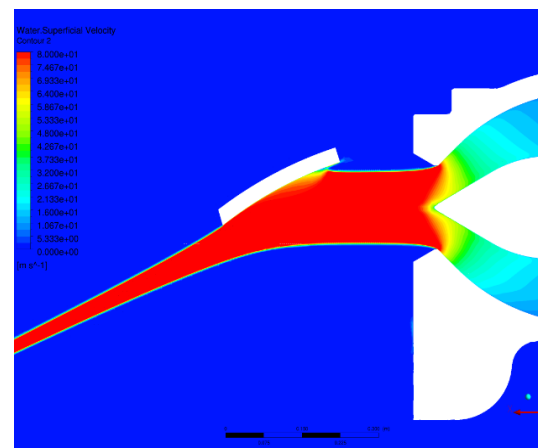


**Figure 5:** Velocity flow field in the nozzle and jet

The velocity distribution in water jet and nozzle for closed deflector position are shown in fig. 5. In the free jet area the shape of the jet is stable with very narrow zone of water-air interference. For the angle  $18^\circ$  of closing position, we have full acceptance of the jet without spilling of the flow over the upper edge of the deflector.

The velocity flow field shown in fig. 5 very clearly determine the “stagnation zone” near the inlet edge of the plate with very low velocity values. The “back flow” is not registered.

Pressure distribution on the top plate surface is shown in fig. 6 where we can see that the maximal values are concentrated in the “stagnation zone”. The distribution is uniform and symmetric. For the most calculation in optimization procedure the deflector geometry was simplified without side walls.

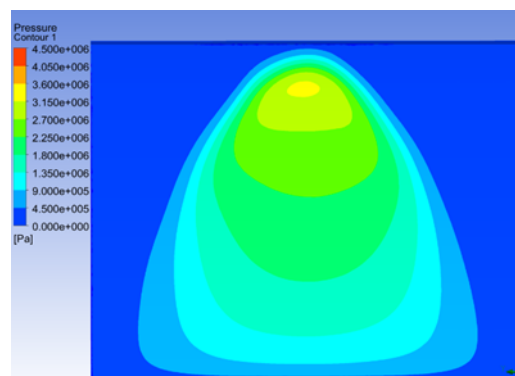


Figure 6: Pressure distribution for basic solution

#### 4.2 Results for different top plate positions

In order to investigate the possibility of reducing the load (hydraulic forces and torque) and angle of closing of the jet deflector, the calculations of kinematic and dynamic parameters, for different angular positions of the top plate were performed. The basic design solution shown in fig. 7 is determined with the angular position of the top plate (chord line) of  $0^\circ$  with respect of the horizontal axis in the open position.

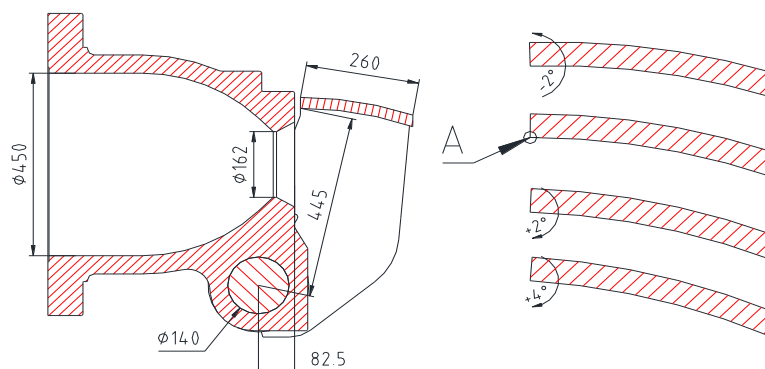
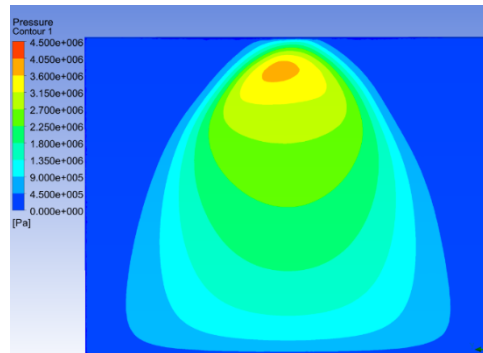


Figure 7: Basic design of the jet deflector in open position and additional geometries of the top plate

Based on the analysis of the basic design, additional three geometries of the deflector in closed position, for angular position of  $-2^\circ$ ,  $+2^\circ$  and  $+4^\circ$  were analysed. The CFD calculations of the flow kinematic and

dynamic parameters were performed for these additional study cases and the comparison of the results was made.

As an example, in the figure 8 the pressure distribution on the top plate surface for angular position of  $+4^\circ$  is shown.



**Figure 8:** Pressure distribution for angle  $+4^\circ$

The comparison of the pressure distribution for all study cases leads to these conclusions:

- The general view of the pressure distribution for all top plate positions is similar.
- The area of high-pressure values (“stagnation zone”) is shifted toward the inlet edge of the plate, as the angular position is of the top plate in higher.
- The value of maximal pressure in “stagnation zone” is higher with respect of higher angular position.

The results of calculated hydraulic torque for all study cases in comparison with the basic solution are specified in table 3.

**Table 3.** The values of hydraulic torque

Position	Mh [kNm]	Difference [%]
$-2^\circ$	11,66	+3,2
$0^\circ$ (basic)	11,30	0
$+2^\circ$	10,67	-5,6
$+4^\circ$	9,91	-12,3

From the comparison of the results in table 3 it is clear that the jet design with angular position of the top plate at  $+4^\circ$  has a lower value of the hydraulic torque for 12,3 percent. Additionally, due to the higher outlet jet angle of this design, the angle of deflector for full closed position of  $18^\circ$  can be reduced for 2 to  $3^\circ$ . This will lead to additional reducing of the hydraulic torque for approximately 8 percent.

### 4.3 The analysis for different top plate geometry

In order to investigate the possibility of further reduction of hydraulic force and torque, investigation has been carried out on various geometry shape of the top plate of the deflector. Modifications of geometry are performed simultaneously in several steps. First, three study cases with variable radius of the curve of the plate including flat plate have been calculated. In order to explore the possibility of reducing the overall load on the deflector construction and the mechanism of the deflector, additional calculations have been made with shortened length of the plate within 25%.

Pressure distribution for flat top plate is given in figure 9 and for top plate with radius of curvature  $R=400$  mm in figure 10.

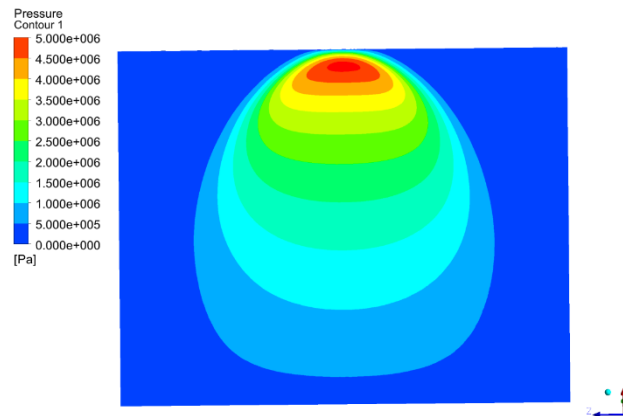


**Figure 9:** Pressure distribution for flat top plate

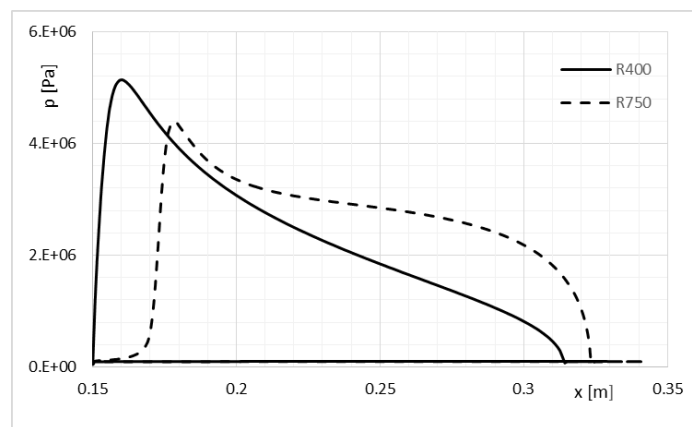


**Figure 10:** Pressure distribution for shortened plate  $R=400$  mm and  $R=750$  mm

From the analysis of the results we concluded as follows:

- the higher radius values lead to higher maximal pressure values and shifting this area toward the leading edge of the plate as we can see from the pressure distribution in figure 9;
- for shortened plate the maximal pressure value is higher (see fig. 10) and deviation angle at the exit is higher for  $6,3^\circ$  to  $8,5^\circ$  in comparison with the basic plate length.

The last modification is made in order to reduce the concentration of high pressure at the input surface. The most convenient technical solution for that purpose is rounded plate in a cross-section, with a part of a cylindrical surface with an appropriate radius. Three radii (see figure 11) for the calculation of the flow parameters values were taken.

As we can see from the figure 12, this solution has two disadvantages: a) due to the roundness of the top plate, the distance between the nozzle and the runner must be higher; b) the dissipation of the water jet at the exit of the deflector is significant.



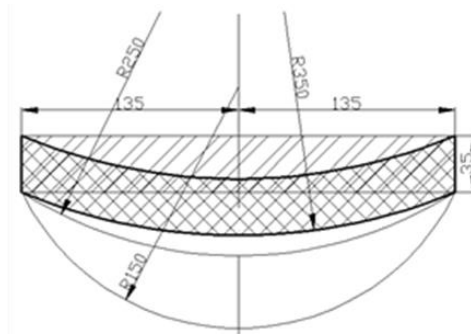


**Figure 11:** Variable radius of the curve of the top plate

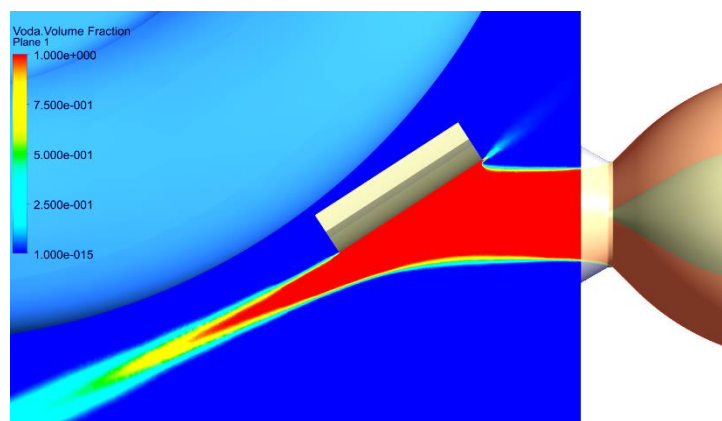


**Figure 12:** Jet cross-section for cylindrical surface of the plate

**Table 4.** Hydraulic forces and torque values of the shortened length of the plate

Modification	$F_x$ [N]	$F_y$ [N]	$F_z$ [N]	$F_R$ [N]	$M_h$ [Nm]
R=750-K	35.489	60.760	2,0	70.366	8.426
R=400-K	35.541	60.715	7,0	70.348	8.420
$r = 350$ mm	34.157	51.740	5	61.999	5.333
$r = 250$ mm	30.781	47.401	6	56.517	4.930

Based on the analysis of the previous presented results in Table 4 the following design solution was selected that fulfilled the set criteria: roundness of the entry surface of the plate with a radius  $r=350$ mm of the cylinder, which continuously crosses into a flat plate toward the exit. Such a defined top plate leads to two additional improvements:

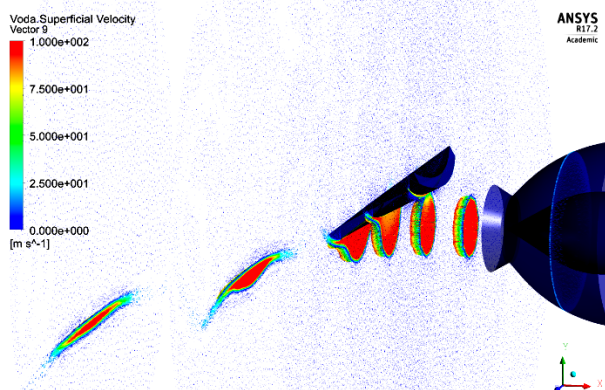
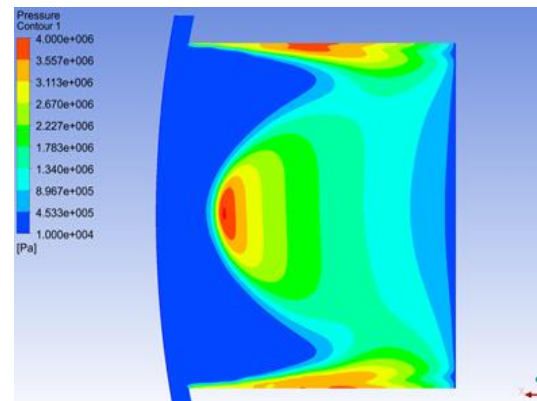
- the height (thickness) of the plate in the area of the outlet edge decreases, which eliminates the need to move the runner shaft for possible sagging in the blades of the runner,
- a homogenization (reduction of dissipation) of the outlet water jet is avoided and the possibility of partial engagement of the jet from the runner blades is eliminated.

The calculation of the hydraulic forces  $F_x$ ,  $F_y$ , and  $F_z$  and torque  $M_h$  for three closing positions  $12^\circ$ ,  $15^\circ$  and  $18^\circ$  (basic solution) of the deflector are performed. The results are specified in table 5.

**Table 5.** Values of hydraulic forces and torque for different closing positions

Case study	$F_x$ [N]	$F_y$ [N]	$F_z$ [N]	$F_R$ [N]	Mh [Nm]
closing position 12°	20.578	41.142	10,0	46.000	5.975
closing position 15°	28.544	50.365	7,0	57.885	6.735
closing position 18°	36.879	57.618	12,0	68.412	6.912

Based on the analysis of the results for three different angles of enclosure, it can be concluded that the exit water jet of the deflector ensures complete deviation of the jet from the trajectory of the blades of the runner with a spare space of 20-25 mm. The position of the deflector determined by a closing angle of 15° is accepted as an optimal technical solution. The shape of the top plate and velocity distributions are given in figure 13 and pressure distribution in figure 14.

**Figure 13:** Velocity distributions in the jet**Figure 14:** Pressure distribution for jet deflector

Finally, the calculation of the basic solution and the final design including the side plates of the deflector was performed. The results of the hydraulic forces and torque are shown in table 6.

**Table 6.** Values of hydraulic forces and torque

Case study	$F_x$ [kN]	$F_y$ [kN]	$F_z$ [kN]	$F_R$ [kN]	Mh [kNm]
Basic solution	42.06	72.19	0.60	83.55	12.45
Final design	36.97	64.58	0.52	74.41	8.99

The comparison of the results in table 6 shows the significant reduction of the hydraulic forces and torque for the final design. Obviously, optimized geometry of the deflector will lead to corresponding significant reduction in strains and deformations.

## 5 Conclusions

From previous experience, different analyses and articles (10), we can conclude that the CFD analysis is sufficiently accurate and precise for more complex applications like the flow in the runner of Pelton turbines and therefore, with great certainty, we can rely on the use in presented case.

Although some simplification is used, the numerical analysis of a Pelton turbine still demands large computing capacities and consumption of excessive CPU time in order to achieve reliable results.

The research for optimization of the top plate geometry of deflector includes investigation of influence of several parameters:

- Angle of the top plate in the open position of deflector,
- Curvature radius of the top plate,
- The chord length of the top plate,
- Curvature radius in the cross-section of the top plate.

Analysis of the calculated flow parameters, hydraulic forces and torque gave as a result selection of the optimal geometry of deflector.

Optimization procedure shows that using different shapes of jet deflector can lead to significant reduction of the hydraulic forces and torque and, consequently to reduction of the servo motor torque. Analysis of different deflector shapes provides information about possible improvements. The final result gives us much useful information for the future research work, where can be used different types of optimisation methods, like multi-objective generic algorithms, etc.

#### References

- [1] Zhang Z., Muggli F., Parkinson E., Schärer C.: *Experimental investigation of a low head jet flow at a model nozzle of a Pelton turbine*, International Seminar Wasserkraftanlagen, Wien, 2000
- [2] Patel K., Patel B., Yadav M., and Foggia T.: *Development of Pelton turbine using numerical simulation*, 25th IAHR Symposium on Hydraulic Machinery and Systems, 2010.
- [3] Zhang Z., Parkinson E., *LDA application and the dual-measurement-method in experimental investigations of the free surface jet at a model nozzle of a Pelton turbine*, 20<sup>th</sup> IAHR Symposium, Charlotte, North Carolina, USA
- [4] Mack R. and Moser W. (2002) *Numerical Investigation of the Flow in a Pelton Turbine*, Proc. of the XXI IAHR Symp. on Hydr. Machin. and Syst. (Lausanne, Switzerland)
- [5] Kvicinsky S., Kueny J.L., Avellan F., Parkinson E.: *“Experimental and numerical analysis of free surface flows in a rotating bucket“*, Proceedings of the 21st IAHR Symposium, Lausanne, Switzerland, 2002
- [6] Parkinson E., Neury C., Garcin H., Vullioud G. and Weiss T. (2005) *Unsteady Analysis of a Pelton Runner with Flow and Mechanical Simulations*, Hydro 2005(Beljak, Austria)
- [7] Perrig A., Avellan F., Kueny J.L., Fahrat M., Parkinson E. (2006). *Flow in a Pelton turbine bucket: numerical and experimental investigations*. J. Fluids Engng.128.
- [8] Bisen D., Shukla S., Sharma P.K., *Optimization and Simulation of Hydro-Turbine Nozzle in Based on Ansys Analysis*, International Journal of Advance Engineering and Research Development, 2014
- [9] Barale D., Limbardi G., Arakerimath R. R., *Modelling and Parametric Fluid Flow Analysis (CFD) and Effect on Convergent Nozzle Used in Pelton Turbine*, Journal of Emerging Technologies and Innovative Research (JETIR), 2016
- [10] Jošt D., Meznar P. and Lipej A., *Numerical prediction of Pelton turbine efficiency*, 25th IAHR Symposium on Hydraulic Machinery and Systems, 2010.
- [11] Popovski B., (2017) *Prediction of the geometry for jet deflector of Pelton turbine in respect of optimal design parameters*, PhD Thesis (University Ss Cyril and Methodius, Faculty of Mechanical Engineering, Skopje, R. Macedonia).